Proc. Natl. Acad. Sci. USA
Vol. 75, No. 2, pp. 573–577, February 1978
Chemistry

Picosecond photodissociation and subsequent recombination processes in carbon monoxide hemoglobin

(picosecond spectroscopy/CO ligand/hemes)

L. J. NOE*, W. G. EISERT†, AND P. M. RENTZEPIS

Bell Laboratories, Murray Hill, New Jersey 07974

Communicated by Hans Frauenfelder, December 2, 1977

ABSTRACT **Excitation of HbCO by a single 6-psec 530-nm pulse results in photodissociation with a first-order constant of 0.89×10^{11} sec^{-1}. The kinetics of photodissociation, monitored by following absorbance changes in the Soret band at 440 nm, are interpreted as corresponding to predissociation followed by a crossing into a dissociative state. Subsequent recombination of CO with the porphyrin system and protein structural transformations were monitored by use of a continuous He-Cd laser beam spatially coincident with the photolysis and Soret interrogation beams at the sample. We find that the latter events take place in three distinct time regions, depending on excitation pulse energy and repetition rate. Excitation of HbCO with a single pulse (0.8–5 mJ) results in a relaxation to the ground state with an associative first-order constant of 5×10^3 sec^{-1}. With a 100-pulse train (~7.5 mJ), a new decay grows with a rate constant of 63 sec^{-1}. For a pulse-train energy of 12 mJ or higher, a delay occurs at the onset of the second (slower) recombination.**

The mechanism describing the cooperative binding of CO and other ligands to Hb poses a fundamental problem that has not been solved quantitatively (1–5). To date, the primary methods used to study cooperative effects have been photodissociation and stopped-flow of a steady state of partially or fully ligated Hb. The subsequent recombination is followed by monitoring optical density changes at suitable wavelengths (6–16). The energetics of ligand-binding in Mb and protoheme have also been investigated by monitoring recombination, after photodissociation, over several orders of magnitude of time (17–19).

The time width of the pulses used for single-pulse excitation cover several ranges: 10–15 μsec with flashlamps (9, 10), about 1 μsec by flashlamp-pumped dye laser (11–13, 18), and 10 msec with Q-switched solid-state lasers (11, 15). Photolysis levels of at least 70% have been reported in most cases.

Because the photodissociation of HbCO provides information on the trigger mechanism for the cooperative binding of ligands to Hb, we thought that a more complete wide-range kinetic investigation of the dissociation and recombination of HbCO would be useful. By photodissociation, we do not necessarily imply the removal of CO from the heme pocket. The present work deseribes the photodissociation of HbCO with a single 6-psec 530-nm excitation pulse from a mode-locked Nd^{+3}-glass laser in conjunction with a second analyzing He-Cd laser. The experimental arrangement allows us to monitor, during the course of an experiment, not only the picosecond photodissociation of HbCO at various wavelengths but also the longer process(es) of protein rearrangement and the recombination of CO with Hb. We find that the photodissociation at 4° initiated by the single excitation pulse at 530 nm takes place in 11 psec and follows first-order kinetics. Subsequent events—recombination of CO and protein structural transformations—take place in three distinct time regions and depend upon excitation pulse energy, pulse repetition rate, and probably, extent of the excitation period.

EXPERIMENTAL

The Hb was prepared from human blood by using standard chromatographic procedures including removal of organic phosphates (20, 21). It was then saturated with CO at 1 atm (1×10^5 Pa) and stored in pellet form (30 g % by weight) in liquid nitrogen. The samples were prepared by diluting a stock solution of melted pellets to a concentration of 240 μM with 0.05 M bis/0.5 M bistris, pH 7.6. This high sample concentration is necessary in order to ensure that the kinetics of the photodissociation and recombination are primarily due to cooperative tetramers rather than to noncooperative dimers (22, 23). A specially designed quartz cell, 1 mm in optical pathlength and 3 cm high, allowed the sample to be thermostated at 5° by circulating coolant through a quartz jacket surrounding the cell (Fig. 1). This cell also was interconnected to a device that provided means for the thermostated 5° 240 μM stock solution of HbCO to be saturated with CO at 1 atm. The solution in the cuvette could be exchanged periodically for fresh stock solution as the need arose.

The photodissociation of HbCO was investigated by using a double-beam picosecond spectrometer described by Netzel and Rentzepis (24). The 6-psec 530-nm excitation pulse is obtained by frequency doubling an amplified 1060-nm pulse selected from the mode-locked train of a Nd^{+3}-glass laser. The average energy of a single 530-nm excitation pulse after amplification is 5 mJ, whereas a nonamplified train of such pulses, 100 pulses per train, at 7-nsec pulse separation contains about 15 mJ. A 530-nm dichroic beam splitter reflects the excitation light to the sample while transmitting the unconverted fundamental 1060-nm light. The unconverted light is then frequency doubled to 530 nm with a second KD*P crystal and used with the remaining 1060-nm light to generate a quasi-continuum in a 20-cm-long cell filled with ethanol. A series of filters (Schott KG3, BG25, and 480-nm short-pass interference) blocks 1060-nm and 530-nm light from the continuum and allows a 200-nm band pass of blue light at 440 nm to reach a quartz echelon constructed of 13 6-psec segments.

After they pass through the echelon, the interrogation beams I and I_0 are formed. The 440-nm interrogation light has the same duration as the excitation light (25) and probes the absorption of any transient or intermediate state(s) created by the

The costs of publication of this article were defrayed in part by the payment of page charges. This article must therefore be hereby marked "*advertisement*" in accordance with 18 U. S. C. §1734 solely to indicate this fact.

* Present address: Department of Chemistry, University of Wyoming, Laramie, WY 82070.
† Permanent address: Institut für Strahlenbotanik, 3000 Hannover-Herrenhausen, Herrenhausen Strasse 2, Germany.

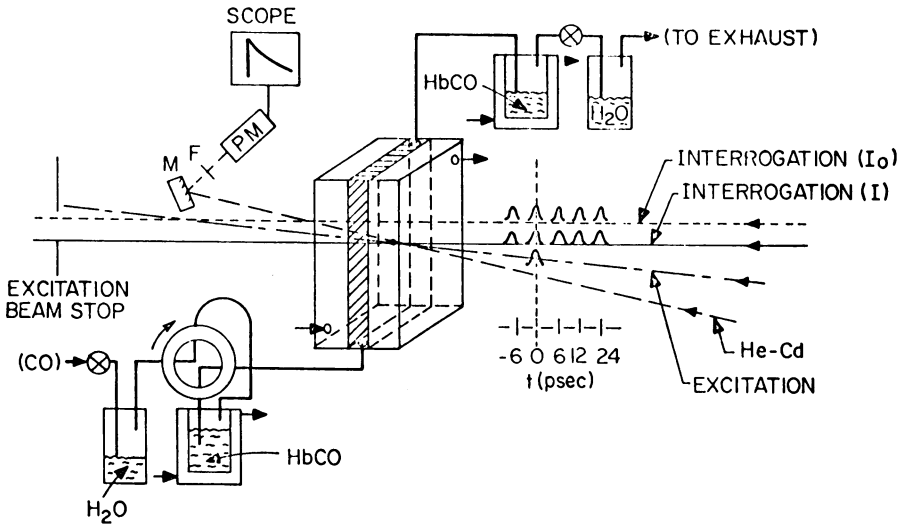

FIG. 1. Diagram of experimental setup, illustrating the spatial interaction of the picosecond continuum and CW He-Cd laser interrogation beams with the excitation beam at the sample cell, the apparatus used for filling the cell and saturating the HbCO solution with CO, and the timing of the 53-nm excitation pulse with the optically delayed continuum pulses (produced by means of an echelon having 6-psec segments) of the double-beam picosecond spectrometer. These I and I_0 beams proceed to a 0.75-m monochromator (not shown) equipped with a silicon-intensified vidicon tube for detection. M, F, and PM identify a mirror, filter, and photomultiplier, respectively, used for detection of absorbance changes at the He-Cd laser wavelength, 441.7 nm. The solid arrows indicate the coolant flow.

530-nm excitation. The excitation pulse is timed to arrive at the sample with one of the interrogation pulses. We monitor the picosecond photodissociation kinetics in the Soret band at 440 nm by using a 0.75-m monochromator coupled to a silicon-intensified vidicon detector. The vidicon detector is interfaced to a computer through an optical multichannel analyzer. After averaging and processing, the data are displayed in the form ΔA, change in absorbance between excitation and no excitation, versus time.

Kinetic processes that occur at times greater than 50 μsec are monitored by a photomultiplier that detects absorbance changes at the He-Cd wavelength, 441.7 nm. These changes are recorded on oscilloscope used in the internal trigger mode. The He-Cd beam is continuously illuminating the sample and is spatially coincident with the 530-nm excitation and probe pulses at the sample, in the configuration shown in Fig. 1. Our data shows that any dissociation initiated by the He-Cd beam is very small and does not affect the results presented in the next section. This statement is supported by the following observations.

(*i*) The observed picosecond kinetics were identical whether or not the He-Cd laser was illuminating the sample.

(*ii*) The optical density is presented as a change, ΔA, and therefore includes a baseline correction that accounts for any possible dissociation caused by the He-Cd beam.

(*iii*) During the course of the picosecond interrogation period, 0–300 psec, the energy available for dissociation, in absolute terms, cannot be larger than 15 pJ, an amount that is negligible compared to the 5-mJ (530 nm) excitation pulse; Similarly, the He-Cd illumination at the 1.25-msec period is equivalent to an energy of 6.25 μJ, again negligible when compared to the 5-mJ excitation pulse.

RESULTS

Fig. 2 shows ΔA versus time t (psec) after a single excitation pulse of approximately 0.8 mJ. The extent of the photolysis, assuming equal probability for photodissociation of different sites (7) assayed by the He-Cd monitor, was approximately 9%. The distribution of intermediates is given by successive terms in the expansion $(p + q)^4$, noting that p is the amount of CO remaining ligated and q is the amount of CO dissociated such that $p + q = 1$. According to this expansion, the 9% of photolyzed HbCO should consist of the following: 86.3% $Hb_4(CO)_3$, 12.8% $Hb_4(CO)_2$, and 0.9% for the remaining dissociated components (7).

Our picosecond kinetic analysis of the photodissociation is based on a three-state system and it assumes a consecutive first-order mechanism

$$A \xrightarrow{k'} B \xrightarrow{k} C.$$

The ground state, A, is $Hb_4(CO)_4$. The intermediates B and C have not been identified although it is quite reasonable to assume that, at the low photolysis levels of this experiment, component C is $Hb_4(CO)_3$. During the course of the experiment we monitored the ΔA as a function of time in the Soret band for the transitions $A \rightarrow A^*$, $B \rightarrow B^*$, and $C \rightarrow C^*$, in which A^*, B^*, and C^* are excited states accessed by the 440-nm probe light, and ϵ_A, ϵ_B, and ϵ_C are the extinction coefficients of these transitions.

When the excitation pulse is treated as a delta function, B will be populated instantaneously with $k' \sim 10^{15}$ sec^{-1}. Because $k' \gg k$, the total ΔA as a function of time, $\Delta A_T(t)$, is the sum of the ΔAs for B and C, $A_0\Delta\epsilon_{BA}e^{-kt}$ and $A_0\Delta\epsilon_{CA}(1 - e^{-kt})$, respectively, in which A_0 is the concentration of molecules excited by the 530-nm pulse and $\Delta\epsilon_{ij}$ is the difference in extinction coefficients between states i and j. The data of Fig. 2 plotted in the linear form, $-\ln[\Delta A_{T\text{-max}} - \Delta A_T(t)]$ versus time is shown in Fig. 3, in which the subscript "max" designates the time of maximum ΔA, result in a first-order rate constant of $(8.9 \pm 0.5) \times 10^{10}$ sec^{-1}. From the intercept and the $\Delta A_{T\text{-max}}$ value, we calculate the ratio $\Delta\epsilon_{CA}/\Delta\epsilon_{BA} = 2.0$ and determine that $\epsilon_C > \epsilon_B$. Using an echelon having longer optical delays, we find that, within experimental error, $\Delta A_T(t)$ remained constant from 42 psec to 0.3 nsec for single-pulse energies in the range 0.8–5 mJ. Within this energy range, k remained constant.

At times greater than 50 μsec, the absorbance data monitored at 441.7 nm within this energy range showed evidence of only one recombination process with a first-order decay rate of 5 ×

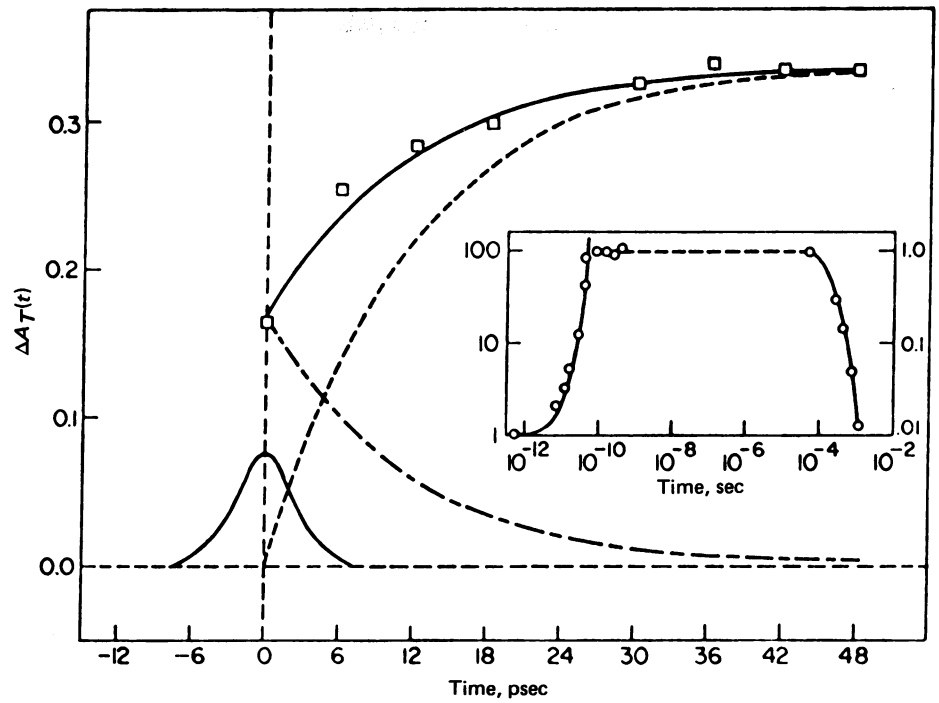

FIG. 2. Absorbance changes in HbCO at 440 nm from $t = 0$ to $t = 48$ psec after single-pulse excitation at 530 mJ. □, Experimental $\Delta A_T(t)$; —, calculated $\Delta A_T(t)$; - - -, calculated $\Delta A_C(t)$; — - —, calculated $\Delta A_B(t)$. The excitation pulse profile is indicated at the origin. The average error in ΔA is ±0.03. (*Inset*) A log-log plot covering 10 orders of magnitude in time, showing the exponential kinetics of both the dissociation and the recombination initiated by a single 530-nm pulse. The left ordinate, $\Delta A_{max}/[\Delta A_{max} - \Delta A_T(t)]$, corresponds to the photodissociation and the right ordinate, $\Delta A(t)/\Delta A_{max}$, corresponds to the recombination. The recombination is in reference to Fig. 3. —, Calculated line; O, experimental points.

10^3 sec^{-1}. This decay is shown in Fig. 3 for a single excitation pulse of approximately 5 mJ. The fast exponential decay is also shown in the *inset* of Fig. 2 along with the picosecond photodissociation kinetics in the form of a log-log plot that spans nine orders of magnitude of time.

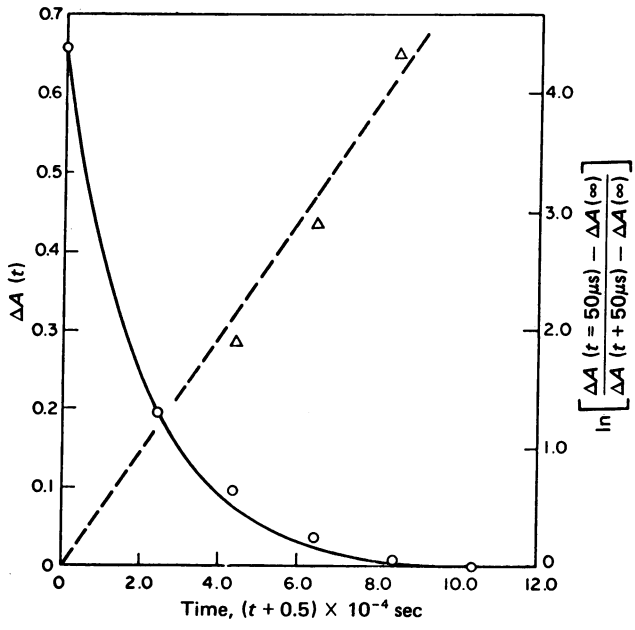

FIG. 3. Absorbance changes in HbCO detected at 441.7 nm as a function of time after excitation. The symbols are observed experimental points; the solid and broken lines are calculated and correspond to $\Delta A(t)$ and the logarithm of $\Delta A(t)$, respectively, for rate $k = (5 \pm 3) \times 10^3$ sec^{-1}. The single-pulse energy was 5 mJ. $\Delta A(\infty)$ refers to the final stable absorbance.

The results with the repetitive pulse train excitation were found to be markedly different than the ones observed for the lower energy single-pulse experiments. At times greater than 50 μsec, the He-Cd monitor revealed the presence of several recombination processes. The decay characteristics of these reassociation process(es) were found to depend on the pulse train energy. With a pulse train energy of 5 mJ, only one recombination process was observed and, as in the single-pulse experiment, it had a first-order rate constant of 5×10^3 sec^{-1}. As the pulse energy was increased, a second, slower, recombination process grew in. At 7.5 mJ, an additional decay was clearly present, with the first-order constant of 63 sec^{-1} shown in Fig. 4. For pulse energies of 12 mJ or higher, a delay appeared at the onset of this second recombination. During this delay there was an increase in ΔA indicative of a third relaxation process. Increase of the excitation energy to 15 mJ resulted in extension of the delay to 15 msec.

DISCUSSION

We interpret the events of the photodissociation initiated by single-pulse excitation at 530 nm by the following three-state mechanism: (*i*) an allowed porphyrin $\pi \rightarrow \pi^*$ excitation (A → B), (*ii*) a predissociation ending at a dissociative state (B → C) (there is a possibility that a triplet state is involved in this step) (26), and (*iii*) dissociation of CO from the heme, which occurs in the range of a vibrational period. This mechanism is in agreement with extended Hückel calculations on iron complexes (27), which suggest that the photodissociation passes through a $d_\pi \rightarrow d_{z^2}$ metal transition in the red spectral region. This dissociative state may be accessed through a level crossing by exciting into an allowed $\pi\pi^*$ porphyrin state, the Q band, lying in the 530-nm region.

The 11-psec lifetime that we observed before the dissociation

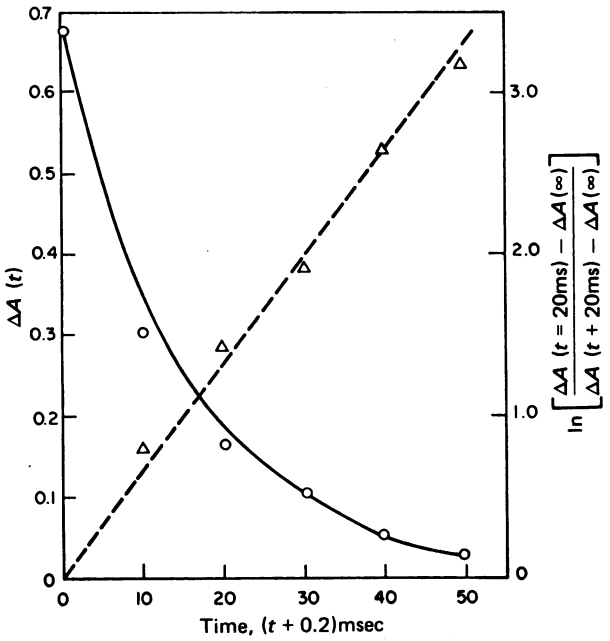

FIG. 4. Rate of recombination of CO with Hb depicted by a dual plot of $\Delta A(t)$ and $\ln\{[\Delta A\ (t = 2\ \text{msec}) - \Delta A(\infty)]/[\Delta A\ (t + 0.2\ \text{msec}) - A(\infty)]\}$ versus time (msec). The data are for the slow recombination process, initiated a 15-mJ excitation. $\Delta A(\infty)$ refers to final stable absorbance. The symbols are observed experimental points; the solid and broken lines are calculated with rate $k = 63 \pm 2\ \text{sec}^{-1}$.

is in disagreement with the 0.5-psec photodissociation reported by Shank *et al.* (16). They used a train of pulses having 0.5-psec time width, nanojoule photon energy, and a repetition rate of one pulse per 100 μsec. This disagreement could be due to the fact that they excited and interrogated with a pulse train at the single wavelength available to them, 615 nm, which is quite close in energy to the dissociative state. The 0.5-psec lifetime they observed could be interpreted as being an upper limit to a fast dissociation. Similarly, a complication could easily arise from the fact that the duty cycle of their excitation pulse is 100 μsec, a time interval much shorter than the recombination lifetime. Therefore, one can envision that they excite and monitor intermediate species rather than only normal ground state HbCO molecules. Our experimental results are entirely different: The 11-psec lifetime is a predissociation and encompasses several relaxation processes including vibrational relaxation and intersystem crossing to the dissociative continuum at ~615 nm.

There are several types of tertiary structural changes possible on the removal of CO from the heme (1, 4, 5). The 0.75-Å displacement of the iron atom out of the plane of the porphyrin is one such possibility. At the present time, we are not able to comment on structural changes of the heme with great certainty. If this displacement occurs subsequent to the dissociation, then it does so with little, if any, spectral change, at least during the time interval 48 psec to 0.3 nsec. Alpert *et al.* (15) proposed that a transient absorption, found during the first 100 nsec after excitation and having a decay constant in the range (0.8–1.8) $\times 10^7\ \text{sec}^{-1}$, was due to a tertiary structural change involving a heme tile. They attributed the major cause of optical changes observed in their work to this structural change. We have not studied this time region (0.3 nsec to 50 μsec) which needs to be carefully probed for additional evidence of (*i*) tertiary structural changes, including the removal of CO from the heme pocket, and (*ii*) the effect of excitation pulse width on structural changes.

At times greater than 50 μsec after excitation with a single pulse in the energy range 0.8–5 mJ, there is a relaxation process that proceeds with first-order or pseudo-first-order rate, $k = 5 \times 10^3\ \text{sec}^{-1}$, to the ground state. In this energy range the extent of the photolysis was between 9% and 50%, corresponding to a solution containing 99–67% total dissociated species of the type $Hb_4(CO)_3$ and $Hb_4(CO)_2$ (7). Considering the percentage of these species, it is likely that, after dissociation, the majority of Hb tetramers are prepared in the R-deoxy state before recombination with CO. Similarly, after dissociation, the removal of CO from the heme pocket is not necessarily complete and subsequent structural changes of the Hb subunits are not expected. Tentatively we suggest that this single relaxation process may be due to R-deoxy Hb combining with CO, probably without structural changes in the subunit. This proposal is supported by the recombination results of recent nitrogen laser experiments in which it was found that a single 1.5-nsec pulse photolyzed approximatley 70% of the sample (28). The subsequent recombination was found to be monophasic with a fast relaxation of several hundred microseconds in duration.

Although one can postulate several possible mechanisms governing the HbCO dissociation and recombination, at present we believe that, even with these data, the process is very complicated and it is premature to assign a mechanism with confidence.

Our pulse-train experiments reflect, depending on the pulse energy, higher degrees of complete photodissociation of the heme sites followed by possible tertiary and quaternary structural changes on recombination. Two recombination processes were observed in the range of 60–80% photolysis whereas three different recombination cases were observed near complete photolysis. In the intermediate energy range it is possible that the kinetics relate to two recombination processes, deoxy-T + CO and deoxy-R + CO, the former displaying a rate constant of $63\ \text{sec}^{-1}$ and the latter, of $5 \times 10^3\ \text{sec}^{-1}$. These slow and fast rates are in good agreement with the corresponding rates, $60\ \text{sec}^{-1}$ and $2.8 \times 10^3\ \text{sec}^{-1}$, reported by Hasinoff (14) who used the ruby fundamental with a pulse duration of ~500 μsec as an excitation source. Depending on the spectral region of interrogation in the Soret band, the biphasic kinetic results of recent photolysis experiments (12, 13) have been interpreted as corresponding to: (*i*) a fast rate due to R-deoxy combining with CO and a slow rate due to T-deoxy combining also with CO, and (*ii*) direct conversion of R-deoxy to T-deoxy as well as CO binding to R-deoxy. The delay in the appearance of the slow recombination in the nearly complete photolysis case may be related to (*i*) the tertiary structural changes of the Hb subunits or (*ii*) quaternary structural transformation, deoxy-R → deoxy-T. It appears that the greater the degree of photolysis, the greater the fraction of slowly recombining Hb observed. Although some of these projections are of a speculative nature at this time, together with the single-pulse results and the data of other workers (12–14) there is an indication that the R → T conformational changes depend on the degree of ligation.

The authors thank Dr. R. Baumann for preparing and supplying us with the Hb samples. We also thank Dr. T. Netzel and Dr. K. Peters for their helpful discussions and Professor Hans Frauenfelder and Dr. L. Eisenstein for valuable discussion and criticism of this manuscript. W.G.E. acknowledges a grant by the German Research Foundation.

1. Baldwin, J. (1975) *Prog. Biophys. Mol. Biol.* **29**, 225–329.
2. Edelstein, S. J. (1975) in *Annual Review of Biochemistry*, eds. Snell, E. E., Boger, P. D., Meister, A. & Richardson, C. C. (Annual Reviews Inc., Palo Alto, CA), pp. 209–232.

3. Monod, J., Wyman, J. & Changeau, J.-P. (1965) *J. Mol. Biol.* **12,** 88–118.
4. Muirhead, H., Cox, J. M., Mazzarella, L. & Perutz, M. F. (1967) *J. Mol. Biol.* **23,** 117–156.
5. Perutz, M. F. (1970) *Nature* **228,** 720–739.
6. Gibson, Q. H. (1956) *J. Physiol. (London)* **134,** 112–123.
7. Gibson, Q. H. (1956) *J. Physiol. (London)* **134,** 123–134.
8. Gibson, Q. H. (1959) *J. Biochem. (Tokyo)* **71,** 293–303.
9. Schmelzer, U., Steiner, R., Mayer, A., Nedetzka, T. & Fasold, H. (1972) *Eur. J. Biochem.* **25,** 491–497.
10. May, R. P. & Mayer, A. (1975) *Eur. J. Biochem.* **52,** 489–593.
11. McCray, J. (1972) *Biochem. Biophys. Res. Commun.* **47,** 187–193.
12. Gray, R. D. (1975) *J. Biol. Chem.* **250,** 790–792.
13. Sawicki, C. A. & Gibson, Q. H. (1976) *J. Biol. Chem.* **251,** 1533–1542.
14. Hesinoff, B. (1974) *Biochemistry* **13,** 3111–3117.
15. Alpert, B., Banerjee, R. & Lindquist, L. (1974) *Proc. Natl. Acad. Sci. USA,* **71,** 558–562.
16. Shank, C. V., Ippen, E. P. & Bershon, R. (1976) *Science* **193,** 50–51.
17. Austin, R. H., Beeson, K., Eisenstein, L., Frauenfelder, H., Gunsalus, I. C. & Marshall, V. P. (1974) *Phys. Rev. Lett.* **32,** 403–405.
18. Austin, R. H., Beeson, K. W., Eisenstein, L., Frauenfelder, H. & Gunsalus, I. C. (1975) *Biochemistry* **14,** 5355–5373.
19. Alberding, N., Austin, R. H., Chan, S. S., Eisenstein, L., Frauenfelder, H., Gunsalus, I. C. & Norlund, T. M. (1976) *J. Chem. Phys.* **65,** 4701–4711.
20. Giuseppe, G., Parkhurst, L. & Gibson, Q. H. (1969) *J. Biol. Chem.* **244,** 4664–4667.
21. Bauer, C. & Pacyna, B. (1975) *Anal. Biochem.* **65,** 445–448.
22. Gibson, Q. H. & Antonini, E. (1967) *J. Biol. Chem.* **242,** 4678–4681.
23. Antonini, E., Anderson, N. M. & Brunovi, M. (1972) *J. Biol. Chem.* **247,** 319–321.
24. Netzel, T. L. & Rentzepis, P. M. (1974) *Chem. Phys. Lett.* **29,** 337–342.
25. Alfano, R. & Shapiro, S. L. (1971) *Chem. Phys. Lett.* **8,** 631–633.
26. Alpert, B. & Lindquist, L. (1975) *Science* **187,** 836–837.
27. Zerner, M., Gouterman, M. & Koboyashi, H. (1966) *Theor. Chim. Acta (Berlin)* **6,** 363–400.
28. Eisert, W. G. (1976) *Annual Index of Current Programs* Vol. 4, B753032; Fifth International Biophysics Congress, 1975 (Copenhagen), abstr. 026650.